

Disclination loops, standing alone and around solid particles, in nematic liquid crystals

E.M. Terentjev

Cavendish Laboratory, Madingley Road, Cambridge, CB3 0HE, United Kingdom

(Received 12 August 1994)

A suspended particle with specific director anchoring on its surface introduces a complex distortion field in a nematic liquid crystal matrix. Topological defects — disclination loops, boojums, and hedgehogs, are needed to match the director near the particle surface with that at the far distance, which is determined by boundary conditions on the sample. This paper analyzes the elastic energy and stability of a singular loop of wedge disclination and the first-order transition of the radial hedgehog into a wide singular loop, driven by an external magnetic field. The far field of distortions, created by a “Saturn ring” of disclination around the spherical radial particle, allows one to calculate the potential of interaction between such particles and with the surface of the liquid crystal. Particles are repelled from each other and from the rigidly anchored surface with the potential $U \sim 1/r^3$. If the sample surface has soft anchoring, the particle is attracted to it at close distances and is repelled, if beyond the anchoring coherence length ξ_w . Several experiments to test these conclusions are suggested.

PACS number(s): 61.30.Gd, 64.60.Cn, 64.70.Md

I. INTRODUCTION

A nematic liquid crystal is uniform in its ground state. Such a state, however, is rarely achieved in practice. On quenching into the phase with broken symmetry, a lot of topological defects appear in the system [1]. The kinetics of the phase transition and properties of the low temperature phase strongly depend on the subsequent behavior of these defects; this problem has a general relevance in condensed matter physics and in cosmology. Topological classification of singularities in liquid crystals, based on homotopy groups in the order parameter space, has been successfully developed [2,3] and the corresponding topological dynamics has been verified experimentally [4,5]. Preceding this work, and in parallel, a lot of research based on continuum director distribution and free energy calculations has been carried out [6,7].

There are two important aspects of the physics of defects — which singularities are topologically stable and, therefore, cannot appear in the system fluctuationally, in isolation. On the other hand, in some constrained geometries the structure with topological defects can be the ground state, and properties of such a state can be distinctly different from those of the uniform one. Constraints on the sample system are most commonly imposed by its boundaries. For example, nematic liquid crystal confined to a spherical droplet with radial (homeotropic) boundary conditions on the director necessarily has a radial point defect (a radial hedgehog) in the middle. A similar droplet with planar conditions would have a bipolar system of boojums [4] (representing the well-known topological problem of “combing the hedgehog”). However, constraints can be imposed by inner boundaries as well. Figure 1 represents the geometry of director distribution around a particle, brought into the liquid crystal matrix. The law of topological charge conservation requires the introduction of additional singularities, which accompany the particle. The type of

these defects depends (as in the droplet) on the kind of surface anchoring — the two limiting cases are drawn in Fig. 1. One can imagine that in most cases the resulting structure will be localized, although sometimes there might be a possibility of introducing strings as well [5,8].

This paper addresses the problem of disclination loops,

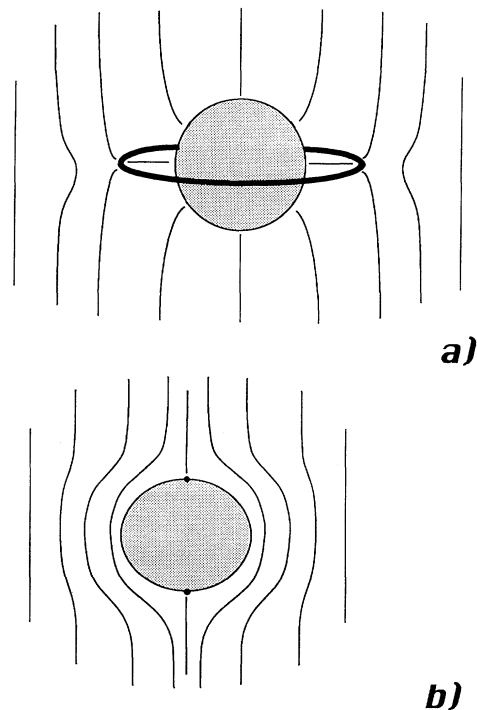


FIG. 1. (a) Particle with radial boundary conditions and a disclination ring in the plane perpendicular to \mathbf{n}_0 . (b) Particle with planar boundary conditions in an otherwise uniform nematic requires a bipolar structure with boojums on poles.

in particular circular rings, which seem to be the most probable scenario after the particle with radial anchoring is brought into the otherwise uniform nematic liquid crystal. This problem has two main aspects, fundamental and practical, and the paper is divided accordingly. Properties, energy, and stability of the disclination loops are important for understanding phase transition kinetics, possibility of monopoles, and topological dynamics. Their relevance is far beyond the specific object of this paper, nematic liquid crystals, and spreads from cosmology to solid state physics. In the next section we shall discuss qualitative, geometrical characteristics of different disclination loops and clarify the distinction between globally singular and nonsingular loops [9]. Section III analyzes the energy of a (globally singular) wedge loop and draws the conclusion that a hedgehog would always be broken into such a (topologically equivalent) loop of characteristic equilibrium radius a^* . Section IV considers the effect of an external orienting field on such a ring disclination. It is shown that a first-order transition takes place on increasing the field along the loop normal, at which the ring expands from its microscopic state with $a^* \sim 10^3 \text{ \AA}$ to the radius R , comparable with the system size. This transition has a wide hysteresis, with critical fields scaling differently with R , and seems to be accessible for experiment.

The last two sections of this paper deal with more practical questions. Foreign particles, suspended in a liquid crystal, have been studied quite extensively, beginning from [10]. Most of these studies [11,12], however, deal with strongly elongated particles (addressing the issue of their ordering) and neglected effects of topological defects. In this paper the director distribution around the radial solid particle [Fig. 1(a)], accompanied by a disclination ring, is approximated and its energy is calculated. The potential energy of interaction between such particles is found to represent anisotropic repulsion, decaying as $1/r^3$ with the distance. Section VI describes the interaction of such particles with the flat boundary of the sample. This interaction strongly depends on the anchoring energy on the boundary: particles are repelled from the surface by image forces if the anchoring is sufficiently rigid. Weak anchoring produces a region of attraction near the surface, which, in practice, may result in depletion layers in particle distribution. These questions may have relevance in several areas of practical applications, which deal with properties of suspensions, because they enable control of the location of external particles in, outside, or near the surface of the volume occupied by nematic liquid crystal. Mixtures of biphasic liquids, or just small volumes of liquid crystal, with surfactant in a micellar state have many internal or external boundaries and, therefore, are also an appropriate object for the present theory.

II. DISCLINATION LOOPS IN NEMATIC LIQUID CRYSTAL

The analysis of disclination loops is relatively simple in the case when a circular loop of a wedge (+1/2) defect is

considered. This represents a special situation when the closed line singularity corresponds to a topological point defect, a hedgehog with the charge (+1) in this case. In the language of the Volterra process [13,14] and orientational Burgers vector Ω , characterizing the disclination, the wedge loop has its local Burgers vector always parallel to the line [the antiparallel configuration represents the (-1/2) loop and would correspond to a (-1) hyperbolic hedgehog]. Consider the process of loop formation in the order parameter space $\mathcal{R}_N = S^2/Z_2$, unit sphere — manifold of orientations \mathbf{n} of a nematic. A stable (1/2) disclination corresponds to a half-circle contour on this sphere with the opposite ends of its arc equivalent through the condition $\mathbf{n} \equiv -\mathbf{n}$. Enclosing the line singularity into a wedge loop corresponds to the rotation of such a contour about its symmetry axis, which corresponds to Fig. 2 with Burgers vector tilt angle $\Theta = \pi/2$. Such process (accounting for $\mathbf{n} \equiv -\mathbf{n}$ condition) covers the whole unit sphere \mathcal{R}_N with a continuous closed surface of points — orientations \mathbf{n} . This, of course, represents a hedgehog point singularity [2,3,5], which has a most significant distortion field: the elastic energy of a hedgehog is linearly proportional to the size of the system, $E_h \sim KR$.

One must note, however, that there are many ways to encircle a loop of a topologically stable (1/2) disclination so that no effective point singularity will occur, and, consequently, the orientational distortions and their elastic energy will remain finite. The classic example has been studied by Friedel and de Gennes in 1969 [15]: the twisted loop, which has its Burgers vector constant

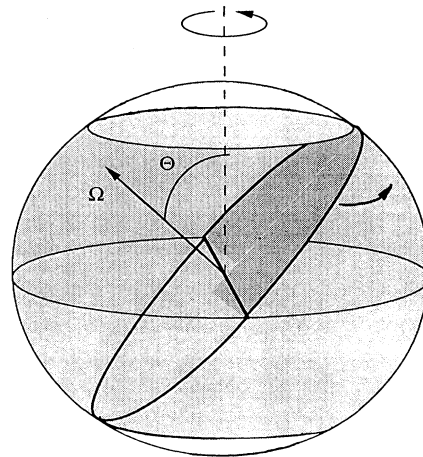


FIG. 2. A process of encircling a loop from a (1/2) disclination in the space \mathcal{R}_N (the disclination is wedge if the line is parallel to the Burgers vector Ω and twist, if perpendicular). The loop is assumed to be in equatorial plane. The key characteristic of the loop is the tilt angle Θ between the local Burgers vector Ω and the loop normal. A singular (wedge) disclination loop corresponds to the full sweeping of \mathcal{R}_N by an initial contour at $\Theta = \pi/2$. Nonsingular loop: at any oblique angle Θ between the loop plane and the Burgers vector the sweeping is not complete and the resulting surface can be contracted to an equatorial circle, $\Theta = 0$ [sic.] topologically unstable twist loop.

and perpendicular to the loop plane (and, therefore, to the disclination line itself). In the order parameter space \mathcal{R}_N this loop corresponds to the rotation of the half-circle (1/2)-disclination contour about the normal to its plane, Fig. 2 with no Burgers vector tilt, $\Theta = 0$. This results in a full circle on the unit sphere \mathcal{R}_N — a distribution \mathbf{n} homotopically equivalent to the uniform state. Accordingly, the energy of the twist loop, which is the opposite limiting case to the wedge one, is found to be limited, $E_t \sim Ka \ln[a/r_c]$ [15], where a is the loop radius and r_c is the disclination core radius. There can be a continuous set of disclination loops between these two limiting cases, when the mutual orientation of the Burgers vector and the line is either fixed, or varies along the loop, but the resulting director distribution $\mathbf{n}(\mathbf{r})$ fails to cover the closed surface covering the order parameter space \mathcal{R}_N , see Fig. 2 for any finite Θ . All such surfaces can be contracted to a circular contour — and ultimately to a point on the unit sphere \mathcal{R}_N , which means that the configuration is still homotopically equivalent to the uniform state. In other words, this means that such intermediate loops can be matched into a uniform director field at far distances and, therefore, can exist in a generally uniform nematic liquid crystal. In contrast, the wedge loop can only exist on its own in a topologically constrained system — the classic example being the spherical droplet of a nematic liquid crystal [4]. Interpolation formula for the loop energy would then take the form $E_l(\Theta) \sim 8\pi KR/[1 + \alpha(R/a) \cos^2 \Theta] + \frac{1}{2}\pi^2 Ka \ln[a/r_c]$, where α is a coefficient of order unity and Θ is the (constant) tilt angle between the Burgers vector $\mathbf{\Omega}$ and the loop normal, Fig. 2.

As we discussed in the Introduction, inserting a particle with rigid boundary conditions on its surface into an otherwise uniform nematic matrix introduces an effective topological singularity, which then has to be compensated by another defect of the opposite charge. A similar situation has been studied by Meyer [16] — spherical air bubbles (with weak anchoring, however) are accompanied by a (-1) hedgehog in the surrounding nematic. Another example of such topological charge conservation, [17], shows that a wedge loop of $(+1)$ disclination [with the overall point charge $(+2)$] is needed to compensate for a hyperbolic (-1) hedgehog in the middle of a radial nematic droplet. In the case we examine here, Fig. 1, the (1/2)-wedge loop will be required to compensate for the long range distortions around the particle. Therefore it is useful to study the properties of such a loop.

III. STABILITY OF THE WEDGE LOOP

The simplest situation is the circular $(+1/2)$ loop, because the symmetry of its director distribution is the same as that of coordinate lines of the ellipsoidal coordinate system [18], Fig. 3 (this concept has also been explored by Mori and Nakanishi [19]). Although in practice, especially for very different values of Frank constants, the director field may be quite different in detail, the ellipsoidal coordinates $\{\sigma, \tau, \phi\}$ give a very plausible analytical ansatz. One can also show that setting $|\hat{\mathbf{n}}_\sigma| = 1$

asymptotically satisfies the equilibrium condition for the nematic, $\mathbf{n} \parallel \nabla^2 \mathbf{n}$, at large distances from the loop (in the one-constant limit for nematic elasticity). It is then straightforward to calculate the total elastic energy of such a defect: taking the disclination core size r_c , radius of the loop $a \gg r_c$ and the “outer radius” of the system $R \gg a$, one obtains in the one-constant approximation $K_1 = K_3 = K$:

$$E_l = \pi K \left[4R + 4R \left(\frac{R}{a} \right) \arctan[a/R] + a \left(\frac{\pi}{2} (1 - \ln[2]) - 6 \arctan[R/a] \right) + \frac{\pi}{2} a \ln[a/r_c] \right] + 2\pi a r_c^2 \mathcal{E}_c,$$

$$E_l \approx 8\pi KR + \frac{\pi^2}{2} Ka \ln[a/r_c] - \frac{\pi^2}{2} Ka \left(5 + \ln[2] - \frac{4}{\pi} \frac{\mathcal{E}_c r_c^2}{K} \right) + \underline{O}(a^2/R), \quad (1)$$

where \mathcal{E}_c is the energy density of the disclination core, which was missing in the paper [19]. Assuming the core is melted, this energy can be qualitatively set as $\mathcal{E}_c \sim U/\xi_N^3$, where U is a characteristic microscopic interaction energy and ξ_N is the nematic correlation length. A natural ex-

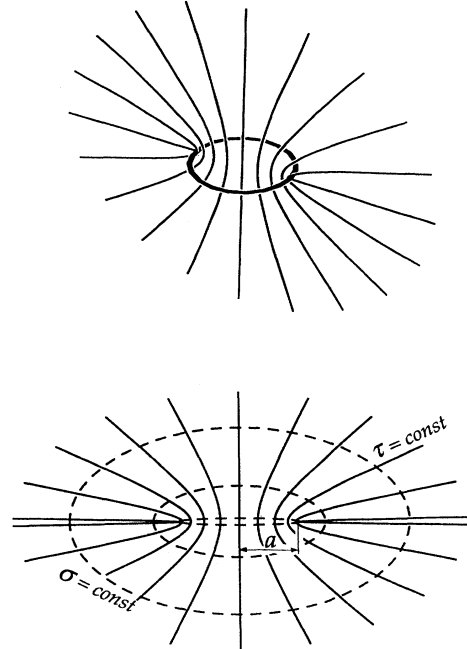


FIG. 3. (a) Director distribution around the circular loop of $(+1/2)$ wedge disclination. (b) Model director field, $\hat{n}_\sigma = 1$, in oblique ellipsoidal coordinates [18].

pectation, that $r_c \sim \xi_N$, leads to a qualitative relation $\mathcal{E}_c \sim Kr_c^2$ and, therefore, the numerical factor in brackets in the second, approximate, expression for E_l is ~ 4.42 .

At large distances from the loop, $R/a \gg 1$, its deformation field and energy correspond to those of a standard radial hedgehog, $8\pi K_1 R$. On this background, additional terms in equation (1) are small corrections. Note, however, that for a nonsingular loop this would be the only relevant contribution to elastic energy.

The question of stability of the radial hedgehog arises from examining the equation (1). Minimizing E_l at $R \rightarrow \infty$ one obtains that the disclination loop has a universal equilibrium radius a^* , given by

$$a^* = r_c \exp \left[4 + \ln[2] - \frac{4 \mathcal{E}_c r_c^2}{\pi K} \right] \sim 30 r_c. \quad (2)$$

For the typical nematic correlation length, $r_c \sim \xi_N \sim 100 \text{ \AA}$, this radius is of the order $a^* \sim 0.3 \mu$. Such a small loop would be practically unobservable by optical methods.

Some interesting possibilities open when one examines extreme limiting cases. Near the transition to the isotropic phase, or to a biaxial nematic, the core energy becomes much smaller, increasing the numerical factor in Eq. (2). Also, in a system with $K_1 \gg K_3$, bend deformations (the loop) are preferable to splay deformations (the hedgehog), and the loop would expand. Such a large splay constant is entirely possible in main-chain nematic polymers and a corresponding microscopic experiment in radial droplets would be of great interest. Another curious region corresponds to smaller "outer radius" R of the radial droplet, where the equilibrium loop size strongly deviates from the universal form (2). In that case a^* becomes dependent on the droplet size, $a^* \sim (Rr_c)^{1/2}$. One has to emphasize once again that all such predictions should be regarded only as qualitative arguments: equations (1) and (2) are valid in a strict mathematical sense only at $K_1 = K_3$ and $R/r_c \rightarrow \infty$.

IV. HEDGEHOG - LOOP TRANSITION IN MAGNETIC FIELD

An obvious way to suppress the radial hedgehog and favor the wide disclination loop is by applying an external field. Consider a spherical volume of nematic liquid crystal with radial boundary conditions. In equilibrium such a system has a radial hedgehog in the middle, or rather a wedge loop, Fig. 3, with a very small radius $a^* \sim 30r_c$. Switching on the magnetic field along the axis of the loop will result in a first-order transition (jump) to a configuration with $a^* \sim R$, the size of the system.

The diamagnetic contribution to the free energy density of a nematic is, as usual [7], $-\frac{1}{2}\chi_a(\mathbf{n} \cdot \mathbf{H})^2$ with χ_a the diamagnetic anisotropy. Substituting n_z given by ellipsoidal coordinates, Fig. 3 [18], and integrating over the sphere, we obtain simply $-\frac{2\pi}{9}\chi_a H^2 (R^3 + 3a^2 R)$. Then the total energy (we keep the one-constant approximation) has the constant contribution, $F_R = 8\pi KR - \frac{2}{9}\pi\chi_a H^2 R^3$, and a part, dependent on the loop radius:

$$\frac{2\Delta F}{\pi^2 KR} \approx \left(\frac{a}{R}\right) \ln[a/R] + \left(\frac{a}{R}\right) \left[\ln[R/r_c] - 5.69 + \frac{4 \mathcal{E}_c r_c^2}{\pi K} \right] - \frac{4}{3\pi} \left(\frac{a}{R}\right)^2 (R^2/\xi_H^2 - 7), \quad (3)$$

where ξ_H is the magnetic coherence length, $\xi_H = (K/\chi_a)^{1/2} H^{-1}$. Equation (3) is an approximation at $a/R \ll 1$ and $a/r_c \gg 1$ and it is useful for the qualitative analysis. For a more exact consideration in the region past the transition, when $a \sim R$, the full loop energy (1) is necessary — its behavior is analyzed numerically and plotted in Fig. 4. One can recognize all features of the first-order transition: the lower critical field H_1 (curve b), when the metastable state at $a \sim R$ first appears, the thermodynamic transition point H^* (curve c), when the two locally equilibrium states have the same free energy, and the upper critical field H_2 (curve d), at which the hedgehog structure [i.e., the small loop with a^* given by Eq. (2)] becomes absolutely unstable.

The lower critical field corresponds to the situation when the maximum of the curve $\Delta F(a)$ is located at $a/R = 1$. This defines the field

$$H_1 \approx \frac{1}{R} \sqrt{\frac{K}{\chi_a}} (C - 0.6)^{1/2}, \quad (4)$$

where the parameter $C = \frac{3\pi}{8} \ln[R/r_c] - \frac{3}{2} \frac{\mathcal{E}_c r_c^2}{K}$. For a typical experiment [5] the nematic droplet size is around 10μ , taking the usual estimate, $\mathcal{E}_c r_c^2 \sim K$, we have $C \sim 8.1$ and $H_1 \sim 2.7(K/\chi_a)^{1/2} R^{-1}$.

The thermodynamic transition field H^* is the point at which $\Delta F|_{a=R} \approx 0$. We obtain

$$H^* \approx \frac{1}{R} \sqrt{\frac{K}{\chi_a}} \sqrt{2} (C - 3.82)^{1/2}; \quad H^* \sim \frac{2.9}{R} \sqrt{\frac{K}{\chi_a}}. \quad (5)$$

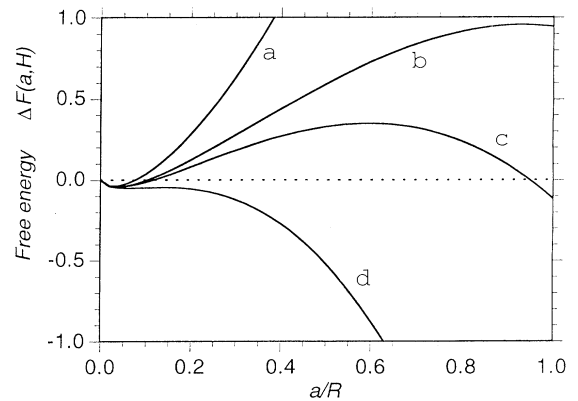


FIG. 4. Free energy (in units $\frac{1}{2}\pi^2 KR$) of the radial droplet in magnetic field, Eq. (3), as a function of the field, a/R , for different characteristic values of the field (see text). Parameter $\chi_a H^2 R^2 / K$ is equal to 0 [curve (a)], 9.5 [curve (b)], 12 [curve (c)], and 20 [curve (d)].

At the upper critical field H_2 , the minimum ($a = a^*$) and the maximum of the free energy (3) merge at $a/R \ll 1$ and $H \gg H^*$. Neglecting complicated effects of transcendental equations for these two extrema, a crude estimate of this condition reads

$$r_c \exp \left[4.69 - \frac{4}{\pi} \frac{\mathcal{E}_c r_c^2}{K} \right] \approx R \frac{C - 5.69}{R^2 / \xi_H^2};$$

$$H_2 \sim \frac{0.3}{(R r_c)^{1/2}} \sqrt{\frac{K}{\chi_a}}. \quad (6)$$

Two critical fields, H_1 and H_2 , determine the ultimate hysteresis width of the droplet switching transition. Since the barrier between the two metastable states at this transition is of the order of $KR \gg k_B T$, it is very likely that the system will remain trapped in each corresponding state for a wide range of fields. This means that on increasing the field, the actual transition (i.e., the loop expansion $a \rightarrow R$) will take place near H_2 , while on decreasing the field, the loop will contract back to the radial structure ($a = a^*$) at a much lower field $\sim H_1$. For a typical nematic droplet with $R \sim 10 \mu$ and magnetic anisotropy $\chi_a \sim 10^{-7}$, these fields have the order of magnitude $H^* \sim 10^3$ Oe and $H_2 \sim 10^4$ Oe. There exists an experiment [20] on the radial droplet switching in external electric field, results of which support the present conclusions.

For all purposes of this paper, the disclination loop in the switched state can be assumed to lie on the droplet surface. In practice, however, the ring may or may not become a surface disclination, depending on the anchoring conditions on the droplet surface. If the nematic anchoring energy W is very large, $K/W \ll \xi_H \ll R$, then the ring will be separated from the surface by a distance $\sim \xi_H$. Anchoring properties will also affect all three characteristic fields. Obviously a more careful analysis of the transition is required to take into account all such effects (see [20] for qualitative discussion and [21] for computer analysis).

V. SPHERICAL PARTICLE WITH HOMEOTROPIC ANCHORING

Bringing a foreign particle with sufficiently rigid homeotropic boundary conditions into an otherwise uniform volume of nematic is equivalent to the creation of an effective topological singularity in its center. Conservation of the topological charge demands the compensation of the corresponding radial hedgehog distribution by an appropriate defect with the total charge (-1) . The most probable scenario is the ring of the wedge $(-1/2)$ disclination, which has a far distortion field similar to that of the hyperbolic hedgehog, Fig. 1.

Calculation of the director distribution for such cylindrically symmetric structure requires adding together the two vector fields, $\mathbf{n}^{(R)}$ for the radial hedgehog and $\mathbf{n}^{(l)}$ for the loop, and renormalizing the result in order to preserve the $|\mathbf{n}| = 1$ constraint. This superposition procedure is allowed in the one-constant elasticity approximation and

for the structures, which have cylindrical symmetry degeneracy of the director fields. In cylindrical coordinates we can write, approximately,

$$n_z^{(R)} = z/r; \quad n_\rho^{(R)} = \rho/r; \quad n_\phi^{(R)} = 0 \quad (7)$$

$$n_z^{(l)} \approx \cos \left(\frac{\pi}{4} - \frac{1}{2} \arctan \frac{\rho - a}{z} \right);$$

$$n_\rho^{(l)} \approx \sin \left(\frac{\pi}{4} - \frac{1}{2} \arctan \frac{\rho - a}{z} \right); \quad n_\phi^{(l)} = 0,$$

with $r^2 = z^2 + \rho^2$ (some care should be taken in order to eliminate the break point on the axis line $\rho = 0$). Similar set of fields corresponds to the other structure with topological charge cancellation: the hyperbolic (-1) hedgehog with a ring of wedge $(+1/2)$ disclination around it. In this case we know the field of the loop to a much greater precision, see Sec. III. In ellipsoidal coordinates we have

$$n_z^{(H)} = \frac{\sigma \tau}{\sqrt{1 + \sigma^2 - \tau^2}}; \quad n_\rho^{(H)} = -\sqrt{\frac{(1 + \sigma^2)(1 - \tau^2)}{1 + \sigma^2 - \tau^2}};$$

$$n_\phi^{(H)} = 0$$

$$n_z^{(l)} = \frac{\tau \sqrt{1 + \sigma^2}}{\sqrt{\sigma^2 + \tau^2}}; \quad n_\rho^{(l)} = \frac{\sigma \sqrt{1 - \tau^2}}{\sqrt{\sigma^2 + \tau^2}}; \quad n_\phi^{(l)} = 0 \quad (8)$$

where $z = a\sigma\tau$ and $\rho = a\sqrt{(1 + \sigma^2)(1 - \tau^2)}$, cf. [18], with the variables in the range $r_c/a < \sigma < \infty$; $-1 < \tau < 1$.

Superposition and renormalization of the fields in (7) or (8) is quite tedious although the result can be presented in a closed form. However, the present analysis has two main purposes: to find the equilibrium radius of the loop around the particle, assuming rigid anchoring conditions, and to obtain the potential of interaction of such particles between each other and with the surface of the liquid crystal. Therefore, the task can be significantly simplified.

In order to determine the loop equilibrium radius it is sufficient to use numerical integration in the one-constant approximation to obtain the energy of the structure described by $\mathbf{n}(\mathbf{r}, a) = (\mathbf{n}^{(R)} + \mathbf{n}^{(l)})/|\mathbf{n}^{(R)} + \mathbf{n}^{(l)}|$. The balance between the loop tendency to contract and reduce the far-field energy and the penalty for violating the rigid anchoring conditions on the particle results in the equilibrium radius of the disclination ring: $a^* \approx 1.8\mathcal{P}$, where \mathcal{P} is the particle size. An obvious interpolation to the general case of finite anchoring strength on this surface gives the optimal separation $a^* - \mathcal{P} \approx 0.8\mathcal{P}/(1 + K\mathcal{P}/W)$. As in Sec. III, this result should be regarded only as a qualitative prediction because the distortion field of the loop $\mathbf{n}^{(l)}$ in (7) and (8) is only valid at $a \gg \mathcal{P}$. Still, the fact that $a^* \sim \mathcal{P}$ will stand in the realistic situation and consistently oriented "Saturn rings" must surround each radial particle in the nematic volume. It would be interesting to compare this prediction with results of an experiment or a computer simulation in order to assess the degree of accuracy of such a crude continuum model.

Interactions with such a particle are determined by its far field of distortions $\mathbf{n}(\mathbf{r})$, which has the simple asymptotic form,

$$n_z = \cos \alpha(\mathbf{r}); \quad n_\rho = \sin \alpha(\mathbf{r}) \quad \text{with} \quad \alpha \approx \frac{\sin 2\theta}{4(r/a)^2}, \quad (9)$$

where θ is the polar angle of spherical coordinates centered in the particle (the angle $\alpha = \frac{1}{2}a^2\rho z/[\rho^2 + z^2]^2$ in proper cylindrical coordinates). In an otherwise uniform nematic all such particles have their rings oriented in the same way, perpendicular to the undistorted director \mathbf{n}_0 . Therefore, it is straightforward to calculate the interaction potential between the two particles separated by a distance d , by superposition of the two fields (9) taken at different origins and integrating the corresponding Frank free energy. This potential represents anisotropic repulsion, proportional to $1/d^3$. When the particles are situated along the symmetry axis $\hat{\mathbf{z}} \equiv \mathbf{n}_0$ of their distortion field, their interaction is

$$U_{\text{int}}(d) \approx \frac{1}{4}\pi^2 K a^4 \frac{1}{d^3}. \quad (10)$$

This expression, as the far field around the particle (9), is asymptotically valid at $d \gg a$.

VI. INTERACTION WITH THE FREE SURFACE

An interesting implication of the above model is the interaction of the foreign particle with the surface of liquid crystal. Consider the semi-infinite volume of uniform nematic with homeotropic (for definiteness) director orientation on its flat surface, in which we have placed a particle with homeotropic coating, analyzed in the previous section. The symmetry axis of the resulting distortion field is perpendicular to the boundary. The outcome of an interaction crucially depends on the anchoring conditions on the nematic boundary. When the director is rigidly locked on this surface, we can use the concept of images and obtain that the particle is repelled from the surface with the potential $U \approx 2\pi^2 K a^4/h^3$, see Eq. (10). Here h is the distance from the surface, $a \sim \mathcal{P}$ is the radius of the disclination ring.

This repulsion can be detected in a simple experiment. Consider the flat homeotropic nematic cell with the bottom plate coated to ensure sufficiently large anchoring energy W_s . Put in small heavy particles, which, given sufficient time, would all sink to the bottom due to the gravity potential $U_g(h) \sim \frac{4}{3}\pi a^3 \Delta\rho g h$ (here, $\Delta\rho = \rho_P - \rho_N$ is the density difference). This force will be balanced by the repulsion of the distortion field and particles will accumulate in the layer, at the equilibrium height,

$$h^* \sim \left(\frac{9\pi K a}{2 \Delta\rho g} \right)^{1/4}. \quad (11)$$

Taking $\Delta\rho \sim 1 \text{ g cm}^{-3}$, $K \sim 10^{-6} \text{ dyn}$ and $a \sim 1 \mu$, we obtain $h^* \sim 10 \mu$. Clearly h^* is not very sensitive to the particle size $\mathcal{P} \sim a$ and will remain in the range of tens of microns for quite a spectrum of particle dimensions, which would make the observation more simple. One might also notice that h^* decreases with the nematic order parameter, $h^* \sim Q^{1/2}$.

The problem of interaction of a defect with the free surface of a liquid crystal, or, in general, a surface with moderate anchoring strength W_s , has been first analyzed by Meyer [16,22] (see, also, the review [23]). In the spirit of that approach in our crude model, we can use the far-field distortions (9), introduce the array of images to compensate for the director deviation on the surface, and integrate the resulting Frank free energy plus the surface energy $\sim W_s \theta^2$. The result is presented in Fig. 5. When the particle is far from the surface, $h \gg \xi_w = K/W_s$, the director on it is virtually undisturbed and the potential is determined by the repulsion from the single image at $d = 2h$, Eq. (10). At $h \ll \xi_w$, the director on the surface is strongly distorted from its equilibrium homeotropic orientation and largely follows the original field (9), created by the particle alone. This results in a situation when the total energy, which is determined now by only a part of the volume accessible for deformations, decreases as this volume decreases, i.e., the particle is attracted to the surface.

A crude approximate of the numerical results on the plot 5 can be made by taking $U(h) \sim 2\pi^2 K a^4/h^3$ at large distances, $h \gg \xi_w$, and linearly increasing $U(h) \sim Ch$ at $h \ll \xi_w$. The coefficient C can be matched at $h = \xi_w$ and is estimated as $C \approx 2\pi^2 K a^4/\xi_w^4$. The energy barrier is, by the same arguments, $\Delta U \sim C\xi_w = 2\pi^2 a^4 W_s^3/K^2$. Given sufficient time for diffusion, all particles within the layer of thickness $\sim K/W_s$ will be attracted to the free surface and accumulated outside the liquid crystalline region.

Another simple experiment could be devised to test these conclusions. Consider the container half-filled with the nematic, which has a flat horizontal free surface (with air, or with a light isotropic liquid). Put in small heavy particles, which would sink through the liquid crystal if there was no potential barrier ΔU . Only very heavy particles, with the density difference $\Delta\rho > \frac{3}{2}\pi K a/g\xi_w^4$ will be able to go over this barrier, lighter ones will remain trapped at the distance $\sim \xi_w$ from the surface by the

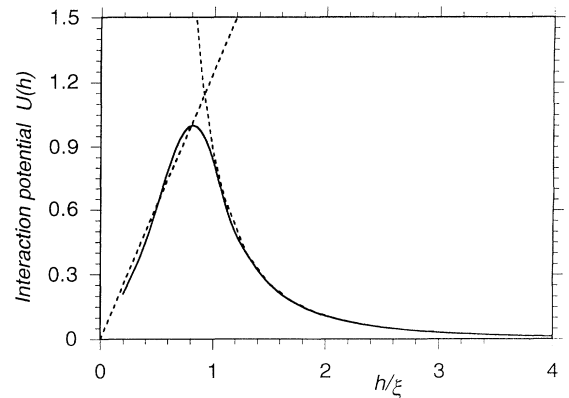


FIG. 5. Potential energy (in units $2\pi K a^4/\xi_w^3$) of interaction between the particle and the homeotropic surface with anchoring strength W_s as a function of separation h/ξ_w from this surface. Parameter $\xi_w = K/W_s$ is the anchoring coherence length. Dotted lines show the approximation by $U \sim 1/h^3$ at large distances and $U \sim h$ at $h/\xi_w \ll 1$.

attraction part of the potential $U(h)$. Taking typical values for weak anchoring energy $W_s \sim 10^{-3}$ erg cm $^{-2}$, Frank constants $K \sim 10^{-6}$ dyn, and particles $a \sim 1 \mu$, we obtain that $\Delta\rho \sim 0.5$ g cm $^{-3}$ is required for separating particles from the surface. If no gravity, or other external field, is involved in such an experiment (for example, when the surface is in the vertical plane), the initial uniform distribution of particles will develop a gap $\sim \xi_w$ near the surface, where all defects will have been attracted and adsorbed to this surface. It is worth noting that at small nematic order parameter Q , the anchoring coherence length $\xi_w \sim Q$ and the barrier $\Delta U \sim 1/Q$, all subject to the applicability of our approximations: $a/h \ll 1$ and $a/\xi_w \ll 1$.

VII. DISCUSSION

This paper has three distinct groups of results and arguments. The discussion in Sec. II has an emphasis on the possibility of topologically unstable disclination loops, depending on the configuration of the local Burgers vector. In fact, all loops, except a narrow class of wedge rings, are homotopically equivalent to the uniform state. This means that their energy is finite and such localized defects (but not “monopoles”) can appear in the system as fluctuations. Such a possibility is especially relevant for the kinetics of the first-order transition after quenching into the nematic phase. Considering conceptual similarities between topological defects in liquid crystals and in various other systems with broken symmetry, such a conclusion may have a wider range of importance.

Sections III and IV target various aspects of the class of topologically relevant wedge disclination loops. The continuum elastic energy analysis of the (+1/2) ring defect is based on the reasonable model for the director distribution, along the coordinate lines of ellipsoidal system. It is shown that the circular loop has an equilibrium radius, a^* of a few thousands Å, i.e., the corresponding radial hedgehog monopole will always be split into the small loop. Note that, although the equilibrium radius a^* is small, it is big enough to satisfy the condition $a \gg r_c$ (the disclination core size), which is necessary for applicability of this continuum approach. The fact that the ansatz, not an exact minimization solution for the director, has been used is not very relevant for our conclusions: had such a solution been known and used, the corresponding free energy would be even lower than (1) and the loop even more favorable. The equilibrium radius a^* exponentially depends on the core energy \mathcal{E}_c of the disclination line. However, it is most likely that the relevant combination, $\mathcal{E}_c r_c^2/K$ is of the order of unity for any model of the core (biaxial, or melted into an isotropic phase, for example) and the result $a^* \sim 30r_c$ is fairly sta-

ble. Such a small radius a^* , probably, will not be seen in any optical experiment, however, the conclusion that true monopoles do not exist in nematic liquid crystals is an important one.

There are ways to make wedge disclination rings bigger: by choosing a material with high elastic anisotropy, $K_1 \gg K_3$, or by applying an external field. Section IV analyzes the first-order transition, the switching of the radial nematic droplet by the magnetic field. At low fields the radial hedgehog (in fact, the small loop with $a = a^*$) structure is demanded by boundary conditions. At sufficiently high field, this loop expands to the radius of the order of the droplet size. This transition is shown to have a very wide hysteresis. In a real experiment (like [20]) the droplet would stay trapped in a corresponding metastable state, making the “switching on” field much bigger than the “off” field.

The last two sections of this paper describe a more practical problem — the behavior of a solid particle, brought into nematic liquid crystal [24]. Radial particles are surrounded by a “Saturn ring” of (1/2) disclination, in the plane perpendicular to the initial uniform director. Qualitative arguments on superposition of director fields show that the radius of such a ring is of the order of the particle size, decreasing when the anchoring on the particle surface becomes weaker. It is shown that such particles interact with each other by means of their distortion fields, the resulting anisotropic repulsion potential is proportional to the inverse cube of separation between the particles. The behavior of micrometer or submicrometer particle suspensions in liquid crystals must be very interesting due to this interaction. Particles not only repel each other, but are repelled from the surface of the sample as well, provided it has sufficiently rigid anchoring. On the other hand, a free surface, or any boundary with weak director anchoring, produces the region of particle attraction with an energy barrier ΔU separating the region of repulsion at far distances. One can imagine applications of such an effect, for example, in a biphasic liquid (with one component mesogenic) suspended particles would avoid going into the liquid crystal but accumulate on its surface. On increasing the temperature above the nematic transition, the described effect would disappear and particles would distribute evenly. The ability to control the location of microscopic particles in a fluid system may have a wide practical significance.

ACKNOWLEDGMENTS

The author benefited from many discussions with O.D. Lavrentovich, A. Lips, P.D. Olmsted, M. Warner, and A.H. Windle. This research has been initiated and supported by Unilever PLC.

- [1] D. Demus and L. Richter, *Textures of Liquid Crystals* (VEB Deutsh. Verlag, Leipzig, 1980).
- [2] G.E. Volovik and V.P. Mineev, *Zh. Eksp. Teor. Fiz.* **72**, 2256 (1977) [*Sov. Phys. JETP* **45**, 1186 (1977)].
- [3] M. Kléman, L. Michel, and G. Toulouse, **38**, L-195 (1977).
- [4] G.E. Volovik and O.D. Lavrentovich, *Zh. Eksp. Teor. Fiz.* **85**, 1997 (1983) [*Sov. Phys. JETP* **58**, 1159 (1983)].
- [5] M.V. Kurik and O.D. Lavrentovich, *Usp. Fiz. Nauk* **54**, 381 (1988) [*Sov. Phys. Usp.* **31**, 196 (1988)].
- [6] F.C. Frank, *Discuss. Faraday Soc.* **25**, 1 (1958).
- [7] P.G. de Gennes and J. Prost, *The Physics of Liquid Crystals* (Clarendon, Oxford, 1993).
- [8] S. Ostlund, *Phys. Rev. B* **24**, 485 (1981).
- [9] V.P. Mineev, in *Soviet Science Review, Section A*, edited by I.M. Khalatnikov (Harwood Academic, New York, 1980), Vol. 2, p. 173.
- [10] F. Brochard and P.G. de Gennes, *J. Phys.* **31**, 691 (1970).
- [11] L. Liebert and A. Martinet, *J. Phys.* **40**, 363 (1979); S.-H. Chen and N.M. Amer, *Phys. Rev. Lett.* **51**, 2298 (1983); B.J. Liang and S.-H. Chen, *Phys. Rev. A* **39**, 1441 (1989).
- [12] S.V. Burylov and Y.L. Raikher, *Phys. Lett. A* **149**, 279 (1990); *Phys. Rev. E* **50**, 358 (1994).
- [13] J. Friedel, *Dislocations* (Pergamon Press, New York, 1964).
- [14] M. Kléman, *J. Phys. Lett.* **38**, L-199 (1977).
- [15] J. Friedel and P.G. de Gennes, *C. R. Acad. Sci. (Paris)* **268**, 257 (1969).
- [16] R.B. Meyer, *Mol. Cryst. Liq. Cryst.* **16**, 355 (1972).
- [17] O.D. Lavrentovich and E.M. Terentjev, *Zh. Eksp. Teor. Fiz.* **91**, 2084 (1986) [*Sov. Phys. JETP* **64**, 1237 (1986)].
- [18] G.A. Korn and T.M. Korn, *Mathematical Handbook* (McGraw-Hill, New York, 1968).
- [19] H. Mori and H. Nakanishi, *J. Phys. Soc. Jpn.* **57**, 1281 (1988).
- [20] V.G. Bondar, O.D. Lavrentovich, and V.M. Pergamenschik, *Zh. Eksp. Teor. Fiz.* **101**, 111 (1991) [*Sov. Phys. JETP* **74**, 60 (1992)].
- [21] S. Kralj and S. Žumer, *Phys. Rev. A* **45**, 2461 (1992).
- [22] R.B. Meyer, *Solid State Commun.* **12**, 585 (1973).
- [23] S. Chandrasekhar and G.S. Ranganath, *Adv. Phys.* **35**, 507 (1986).
- [24] P. Poulin, V.A. Raghunathan, P. Richetti, and D. Roux, *J. Phys. II (France)* **4**, 1557 (1994).

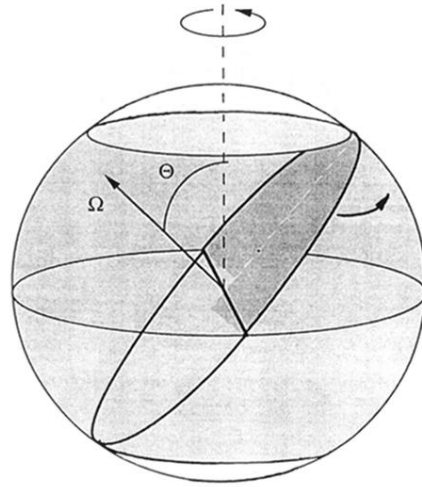


FIG. 2. A process of encircling a loop from a $(1/2)$ disclination in the space \mathcal{R}_N (the disclination is wedge if the line is parallel to the Burgers vector Ω and twist, if perpendicular). The loop is assumed to be in equatorial plane. The key characteristic of the loop is the tilt angle Θ between the local Burgers vector Ω and the loop normal. A singular (wedge) disclination loop corresponds to the full sweeping of \mathcal{R}_N by an initial contour at $\Theta = \pi/2$. Nonsingular loop: at any oblique angle Θ between the loop plane and the Burgers vector the sweeping is not complete and the resulting surface can be contracted to an equatorial circle, $\Theta = 0$ [sic.] topologically unstable twist loop.